Enhanced Hydrogenation in a Reverse Flow Chromatographic Reactor

Guillermo A. Viecco, Brad J. Carnish, and Hugo S. Caram
Dept. of Chemical Engineering, Lehigh University, 111 Research Drive, Bethlehem, PA 18015

DOI 10.1002/aic.10779
Published online February 1, 2006 in Wiley InterScience (www.interscience.wiley.com).

An experimental study of the reverse flow chromatographic reactor is carried with the equilibrium limited hydrogenation of 1,3,5-trimethylbenzene (mesitylene, MES) to 1,3,5-trimethylcyclohexane. The reaction is pseudo first-order when carried out in excess hydrogen. A simple experimental setup is used to evaluate the effects of carrier flow, reactant feed concentration, and amount of catalyst on conversion. Conversions exceeding the thermodynamic equilibrium conversion are obtained for a wide variety of switching times, catalyst amounts, carrier flow rates, and reactant concentrations, showing the robustness of the system. While the qualitative features of the process can be predicted for a simple linear adsorption equilibrium model, the experimental results are best fitted by assuming a linear adsorption isotherm combined with an adjusted interfacial mass-transfer resistance. The experimental results are very similar to those reported in previous research of the same reaction in a simulated moving-bed chromatographic reactor.
 AIChE J, 52: 1855–1865, 2006
Keywords: reactive separation, hydrocarbon hydrogenation, chromatographic reactor, dynamic operation, reverse flow

Introduction

The reverse flow chromatographic reactor (RFCR) is a fixed-bed reactor packed with an admixture of adsorbent and catalyst, where at least one of the reactants is fed at the middle of the reactor, and where the flow direction of the carrier is periodically switched according to Figure 1. If the adsorbent has a high adsorption capacity toward the reactant, and low toward the products, the periodic switching of the carrier can be used to trap the strongly-adsorbed reactant inside the reactor.

The value of the RFCR can be illustrated for the equilibrium-limited first-order reaction $A \rightleftarrows B$. Since the adsorbent has lower adsorption capacity toward the product than the reactant, the products are swept away, inhibiting the reverse reaction and allowing a higher overall conversion than the thermodynamic steady-state equilibrium value. The slow rate of propagation of the reactant allows the concentration inside the reactor to be higher than that of the feed concentration, thereby increasing the effective forward reaction rate. Thus, a smaller reactor or a smaller amount of catalyst is required to achieve the same conversion than in any other type of conventional steady-state reactor.

Agar and Ruppel (1988) and Falle et al. (1995) have previously studied the RFCR. Their study was limited to a first-order irreversible reaction, the selective catalytic reduction (SCR) of NOx by NH_3, where only ammonia is adsorbed and is the reactant fed at the middle of the reactor. By using the RFCR, complete conversion of NOx was predicted with little or no slip of ammonia from the system. The system was assumed to only adsorb ammonia and not any of the other products or reactants, and great attention was invested in determining the shape and velocity of the ammonia wave to determine the frequency with which the flow direction should be changed. More recently, Jeong and Luss (2003) revisited this problem providing a more detailed mathematical analysis, while Viecco and Caram

Correspondence concerning this article should be addressed to H. S. Caram at hsc0@lehigh.edu.

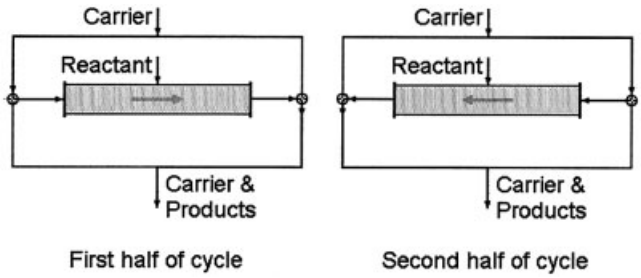

Figure 1. RFCR.

(2004) have shown that the RFCR can significantly improve conversion for equilibrium-limited reactions. Little or no experimental information is available for the RFCR.

Previous studies of the countercurrent moving chromatographic reactor, CMCR (Fish and Carr, 1989), and the simulated moving-bed chromatographic reactor, SMBCR (Ray and Carr, 1995) have shown the need to carry out experimental investigation of such systems to verify the validity of the numerical simulation results. As part of this work, a numerical model with an analytical solution has been developed, and it has been shown that the RFCR can significantly enhance the conversion above the thermodynamic equilibrium values.

Mathematical Model

An evaluation of the performance of the reactor can be obtained by modeling the RFCR (or the SMBCR) as a chain of N continuous stirred-tank reactors (CSTR), as shown in Figure 2. The tank-in-series model has been used to represent two effects, the axial mixing and the interfacial mass-transfer resistance between the solid and fluid phase, since both will appear as axial dispersion. Most of the calculations have been made using 51 tanks, since a larger number of tanks does not seem to affect the conversion response, and a plug flow is being approximated. The model assumes that the reactor is isothermal with negligible pressure drop, and the reactant is fed at the $^{(N+1)}/_{2}$ CSTR. The complete cycle is split into a forward cycle, where carrier fluid enters at the 1st CSTR and leaves at the Nth CSTR, and a reverse cycle. Three models will be presented here: an analytically-solved linear model, a numerically-solved kinetic model that will approximate a competitive Langmuir isotherm, and an analytical linear model based from the Langmuir one that will include mass-transfer resistance.

Simple linear model

The first model is derived assuming that a local adsorption equilibrium between the two phases exists at each stage, and that the adsorption equilibrium can be described by the linear adsorption isotherm, $n_{A,i} = K_A C_{A,i}$ (neglecting the amount adsorbed in the catalyst). When no feed is added to the stage, the material balance in the ith stage, for a first-order reversible reaction ($A \rightleftarrows B$), occurring with constant flow rate, is

$$\varepsilon V_i \frac{dC_{A,i}}{dt} + (1-\varepsilon) V_i \frac{dn_{A,i}}{dt} = q(C_{A,i-1} - C_{A,i}) - V_i k_f \left(C_{A,i} - \frac{C_{B,i}}{K_e} \right) \quad (1a)$$

$$\varepsilon V_i \frac{dC_{B,i}}{dt} + (1-\varepsilon) V_i \frac{dn_{B,i}}{dt} = q(C_{B,i-1} - C_{B,i}) + V_i k_f \left(C_{A,i} - \frac{C_{B,i}}{K_e} \right) \quad (1b)$$

or in dimensionless variables as

$$\frac{dC_{A,i}}{d\tau_i} = C_{A,i-1} - C_{A,i} - Da_i \left(C_{A,i} - \frac{C_{B,i}}{K_e} \right) \quad (2a)$$

$$\frac{dC_{B,i}}{d\tau_i} = \gamma \left[C_{B,i-1} - C_{B,i} + Da_i \left(C_{A,i} - \frac{C_{B,i}}{K_e} \right) \right] \quad (2b)$$

where

$$K_i' = \varepsilon + (1-\varepsilon) K_i \quad (i = A, B) \quad (3a)$$

$$\gamma = \frac{K_A'}{K_B'} \quad (3b)$$

$$\tau_i = \frac{tq}{K_A' V_i} \quad (3c)$$

$$Da_i = \frac{V_i k_f}{q} = \frac{Da}{N} \quad (3d)$$

where τ_i represents the apparent residence time of the reactant in the ith stage. For N stages with the same volume, the resulting system of ODEs can be written in matrix form as

$$\frac{d\mathbf{C}}{d\tau_i} = \mathbf{AC} + \mathbf{F} \quad (4)$$

For initial conditions given by $\mathbf{C}_0$, and feed conditions given by $\mathbf{F}$, the solution to this problem is widely known:

$$\mathbf{C}(\tau_i) = e^{\mathbf{A}\tau_i}\mathbf{C}_0 + [e^{\mathbf{A}\tau_i} - \mathbf{I}]\mathbf{F} \quad (5)$$

where the feed vector $\mathbf{F}$ is

$$\mathbf{F} = \begin{bmatrix} 0 \\ \vdots \\ 0 \\ C_{A0} \\ 0 \\ \vdots \\ 0 \end{bmatrix} \leftarrow \frac{N+1}{2} \quad (6)$$

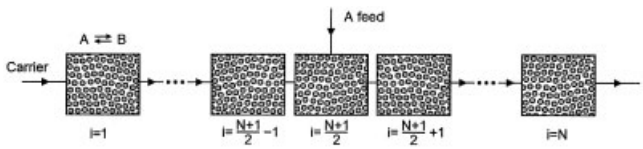

Figure 2. RFCR represented as a series of CSTRs.

The feed concentration, C_{A0}, is defined as

$$C_{A0} = \hat{n}_A/q \tag{7}$$

where $\hat{n}_A$ is the molar feed rate of reactant A at the $^{(N+1)}/_2$ stage.

An analytical solution is possible, when the cyclic steady state is considered. For the RFCR, the concentration profile at the end of half a cycle is the mirror image of that at the beginning of the cycle. Therefore

$$\mathbf{C}_0(\tau_i) = \mathbf{M}\mathbf{C}_0(\tau_i + \delta\tau_i) \tag{8}$$

where $\delta\tau_\iota$ is the dimensionless half cycle time, and $\mathbf{M}$ is the mirror matrix given by

$$\mathbf{M} = \begin{bmatrix} 0 & & 1 \\ & \iddots & \\ 1 & & 0 \end{bmatrix} \tag{9}$$

Substituting Eq. 8 into 7, and rearranging the initial concentration at the cyclic steady state is then given by

$$\mathbf{C}_0 = [\mathbf{M} - e^{\mathbf{A}\delta\tau_i}]^{-1}\mathbf{A}^{-1}[e^{\mathbf{A}\delta\tau_i} - \mathbf{I}]\mathbf{F} \tag{10}$$

Finally, the average concentration in the reactor, including the reactor exit concentration, is given by

$$\mathbf{C}_{average} = \frac{1}{\delta\tau_i}\int_0^{\delta\tau_i} \mathbf{C}(\tau_i)d\tau_i = \frac{\mathbf{A}^{-1}}{\delta\tau_i}[e^{\mathbf{A}\delta\tau_i} - \mathbf{I}]\mathbf{C}_0 + \frac{\mathbf{A}^{-2}}{\delta\tau_i}[e^{\mathbf{A}\delta\tau_i} - \mathbf{I}]\mathbf{F} - \mathbf{A}^{-1}\mathbf{F} \tag{11}$$

The dimensionless switching time used in the development of the model, $\delta\tau_i$, can be more conveniently written as

$$\delta\tau^* = \frac{t_s q}{K'_A V} = \frac{tq}{K'_A N V_i} = \frac{\delta\tau_i}{N} \tag{12}$$

which allows for direct comparison of the results regardless the number of stages, and keeps the dimensionless switching time as an independent dimensionless variable.

Langmuir model

The linear model assumes an infinite capacity of the adsorbent and local equilibrium, as well as no competition between products and reactants for the adsorbent sites. A more realistic model should assume a Langmuir competitive adsorption isotherm and account for a gas-solid mass-transfer resistance. Such a model can be expected to describe more accurately industrial conditions where the adsorbent and catalyst inventories must be minimal and the product output maximum. A competitive Langmuir adsorption isotherm for the jth component is given by

$$\frac{n_j}{c_{max}} = \frac{K_j^{ads}c_j}{1 + \sum K_k^{ads}c_k} \tag{13}$$

Because of the difficulty in handling this type of isotherm it is convenient to use the pseudokinetic approach. Under this approach, the material balances for the i[th] stage during the forward half of the cycle for an equilibrium limited reaction of the type $A \rightleftarrows B$ are given by

$$V_i\varepsilon\frac{dc_{A,i}}{dt} = q(c_{A,i-1} - c_{A,i}) - V_i(1-\varepsilon)k_{ads}c_{\max}\left(\theta_i c_{A,i} - \frac{\theta_{A,i}}{K_A^{ads}}\right) - k_p\varepsilon V_i\left(c_{A,i} - \frac{c_{B,i}}{K_e}\right) \tag{14a}$$

$$V_i\varepsilon\frac{dc_{B,i}}{dt} = q(c_{B,i-1} - c_{B,i}) - V_i(1-\varepsilon)k_{ads}c_{\max}\left(\theta_i c_{B,i} - \frac{\theta_{B,i}}{K_B^{ads}}\right) + k_p\varepsilon V_i\left(c_{A,i} - \frac{c_{B,i}}{K_e}\right) \tag{14b}$$

$$V_i(1-\varepsilon)\frac{dn_{A,i}}{dt} = V_i(1-\varepsilon)k_{ads}c_{\max}\left(\theta_i c_{A,i} - \frac{\theta_{A,i}}{K_A^{ads}}\right) \tag{14c}$$

$$V_i(1-\varepsilon)\frac{dn_{B,i}}{dt} = V_i(1-\varepsilon)k_{ads}c_{\max}\left(\theta_i c_{B,i} - \frac{\theta_{B,i}}{K_B^{ads}}\right) \tag{14d}$$

where the fraction of free adsorption sites given by

$$\theta_{j,i} = \frac{n_{j,i}}{c_{\max}} \tag{15a}$$

$$\theta_i = 1 - \vartheta_{A,i} - \vartheta_{B,i} \tag{15b}$$

Equations 14a–d can be made dimensionless to obtain

$$\frac{dC_{A,i}}{d\tau^+} = C_{A,i-1} - C_{A,i} - vDa_{ads}\left(\theta_i C_{A,i} - \frac{\theta_{A,i}}{K_A^{ads}c_0}\right) - Da\left(C_{A,i} - \frac{C_{B,i}}{K_e}\right) \tag{16a}$$

$$\frac{dC_{B,i}}{d\tau^+} = C_{B,i-1} - C_{B,i} - vDa_{ads}\left(\theta_i C_{B,i} - \frac{\theta_{B,i}}{K_B^{ads}c_0}\right) + Da\left(C_{A,i} - \frac{C_{B,i}}{K_e}\right) \tag{16b}$$

$$\frac{d\theta_{A,i}}{d\tau^+} = Da_{ads}\left(\frac{c_0}{c_{\max}}\right)\left(\theta_i C_{A,i} - \frac{\theta_{A,i}}{K_A^{ads}c_0}\right) \tag{16c}$$

$$\frac{d\theta_{B,i}}{d\tau^+} = Da_{ads}\left(\frac{c_0}{c_{\max}}\right)\left(\theta_i C_{B,i} - \frac{\theta_{B,i}}{K_B^{ads}c_0}\right) \tag{16d}$$

Where the dimensionless variables and parameters are defined as

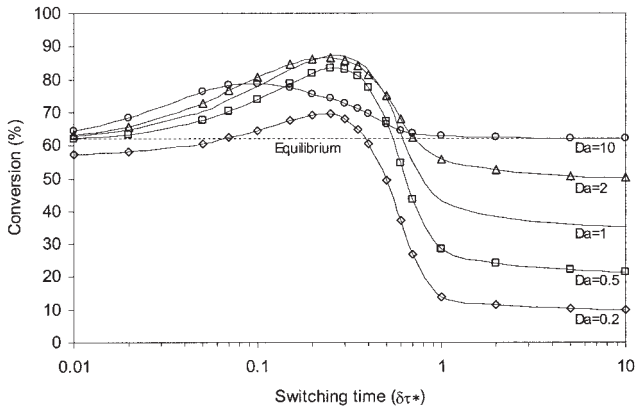

Figure 3. Conversion as a function of the switching time for an equilibrium limited reaction (K_e = 1.63, γ = 3, N = 61).

$$\tau^{+} = \frac{tqN}{\varepsilon V} \tag{17a}$$

$$C_{j,i} = \frac{c_{j,i}}{c_0} \tag{17b}$$

$$\theta_{j,i} = \frac{n_{j,i}}{c_{\max}} \tag{17c}$$

$$Da_{ads} = \frac{V_i \varepsilon k_{ads} c_{\max}}{q} \tag{17d}$$

$$\upsilon = \frac{1-\varepsilon}{\varepsilon} \tag{17e}$$

Notice that the dimensionless time τ^{+} differs from the dimensionless time τ_i, defined before since it does not include the linear adsorption constant K_A'. This mathematical model also considers that the reaction rate is linear and can be expressed in terms of the gas phase concentration. Although this is not true in most industrial applications, it indicates that the reaction does not take place on the surface of the adsorbent, and it allows comparison of the effect of the adsorption isotherm separately from the reaction. The extended model contains four new parameters: Da_{ads}, (c_0/c_{max}), $K_A^{ads}c_0$, K_b^{ads} $c_{0,}$ but the separation factor γ has been eliminated. To reduce the number of calculations two asymptotic cases will be considered. For this kinetic model, the gas and adsorbent concentrations are not at equilibrium in each stage. To approximate local adsorption equilibrium so that all the models can be compared, the adsorption rate dimensionless constant Da_{ads} was increased until the resulting concentration profiles became insensitive to the value of Da_{ads}. Therefore, the gas and adsorbent concentrations were almost at the adsorption equilibrium, effectively reducing the number of additional parameters included to two.

Linear mass-transfer model

It is also possible to maintain the linear isotherm approximation, but include the effect of the mass-transfer resistance. This is done by assuming an unlimited capacity of the adsorbent (θ_i =1) in the Langmuir model, which has the advantage of allowing for an analytical solution similar to that presented for the linear equilibrium model. However, a complete analysis of these models is beyond the scope of this article and their application will only be presented in the context of the experimental results.

Numerical Simulations

The simple linear model for equilibrium limited reactions has five dimensionless parameters: the Damkohler number Da; the switching time $\delta\tau^*$; the number of equilibrium stages N; the equilibrium constant k, and the separation factor γ. This part of the discussion will be limited to the linear model without an interfacial mass-transfer resistance. The first two parameters studied were the switching time and the Damkohler number. Figure 3 shows the conversion as a function of the switching time for a variety of Damkohler numbers. There is a wide range of both switching times and Damkohler numbers that yield in improved conversion over the thermodynamic equilibrium, and there is a switching time and Damkohler number that maximizes the conversion. From moderate switching times ($\delta\tau^*<0.6$), the conversion exceeds the thermodynamic equilibrium for all but the smaller Damkohler numbers. This is the result of the trapping of both reactant and product at low switching times ($\delta\tau^*<0.01$), and since there is a slightly larger escape of product than reactant, the conversion slightly exceeds the thermodynamic equilibrium conversion.

At large switching times, the conversion depends on the Damkohler number, since the reactor is essentially behaving as a plug-flow reactor (PFR) of half the Damkohler number. Therefore, large Damkohler numbers (Da $>$ 5) yield a conversion approaching the equilibrium conversion. The range of switching times where the conversion is improved over the thermodynamic equilibrium, $\delta\tau^*<0.7$, shows the robustness of the system. The presence of an optimum Damkohler number, which maximizes the conversion is somewhat unexpected. For conventional reactors, larger reactors in equilibrium-limited reactions always mean larger conversion. In the RFCR, the optimum Damkohler number is fairly small, Da = 1.5, as observed in Figure 4, where the maximum conversion is plotted as a function of the Damkohler number. The PFR conversion for this Damkohler number with the same equilibrium

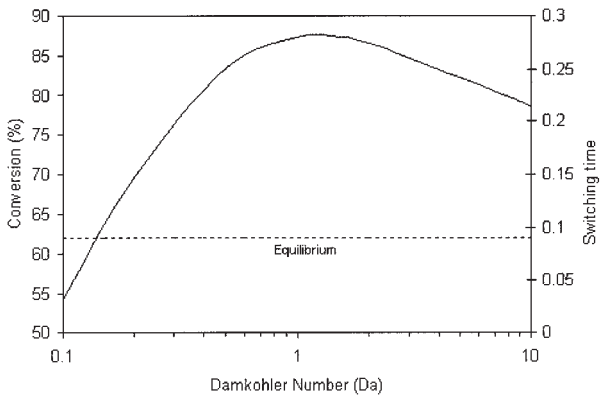

Figure 4. Maximum conversion as a function of the Damkohler number (K_e = 1.63, γ = 3, N = 61).

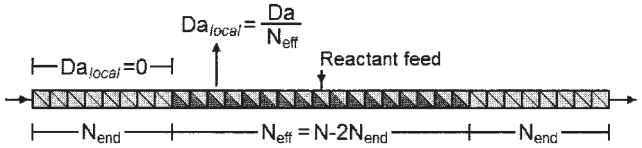

Figure 5. RFCR with a structured packing configuration.

constant is 52%, much smaller than the 87.3% conversion obtained at the optimum switching time ($\delta\tau^* = 0.25$). For very large Damkohler numbers, and no structured catalyst, the conversion will approach equilibrium regardless of the switching time, as observed for Da = 10 in Figure 3.

A study of the concentration profile showed that it was advantageous to remove the catalyst from the end sections of the RFCR. This structured packing configuration is modeled by setting the local Damkohler number to 0 for N_{end} equilibrium stages at each end of the RFCR. For the remaining equilibrium stages, the local Damkohler number is given by

$$Da_{local} = \frac{Da}{N_{eff}} \tag{18}$$

where $N_{eff} = N - 2N_{end}$ is the effective number of CSTRs or equilibrium stages that contain catalyst. This packing configuration is shown in Figure 5.

Figure 6 shows the conversion for an equilibrium-limited reaction using different packing configurations. The packing configuration is expressed by the number of effective equilibrium stages with catalyst N_{eff}. At very low switching times, the best performance is obtained when all stages have catalyst. At intermediate switching times, where the maximum conversion is obtained, there is a structured packing scheme which significantly improves the conversion over that obtained in a RFCR with catalyst in all stages. Figure 7 shows the maximum conversion for a fixed reactor size, calculated using Eq. 11, obtained at a switching time of 0.25 as a function of the fraction of reactor with catalyst (N_{eff}/N). This figure clearly shows the appreciable improvement in conversion that can be

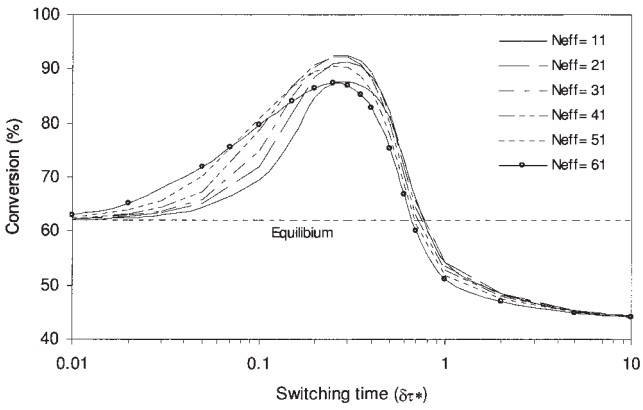

Figure 6. Conversion as a function of the switching time for different catalyst packing configurations in an equilibrium limited reaction for Da = 1.5, N = 61, γ = 3, K_e = 1.63.

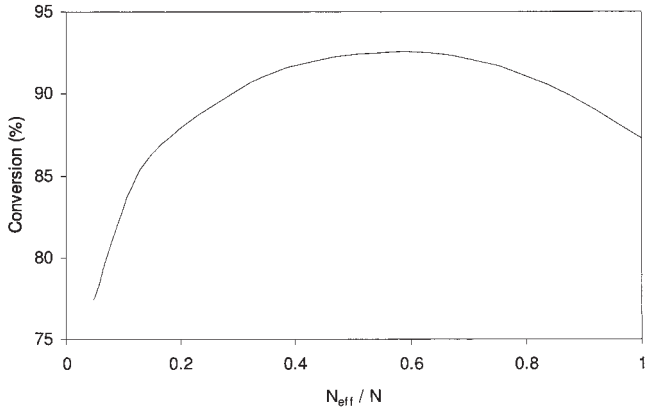

Figure 7. Conversion as a function of the packing configuration, Neff/N ($\delta\tau^*$ = 0.25, Da = 1.5, N = 61, γ = 3, K_e = 1.63).

obtained with the RFCR, and how using a simple structured packing configuration can improve the conversion.

The maximum conversion obtained for an equilibrium conversion of 62% and 61 total equilibrium stages was at N_{eff} = 31, which yielded in an increase in conversion from 87.3 to 92.6% at a switching time of $\delta\tau^* = 0.3$. If the local Damkohler number in each equilibrium stage is kept constant, the total amount of catalyst can be reduced and improvement in conversion can be obtained. For 61 equilibrium stages, conversion jumps from 87.3% to 90.9% for a system with Da_{local} = 1.5/61 = 0.0164, and N_{eff} = 31 at a switching time of $\delta\tau^*$ = 0.3. Using small sections with very large amounts of catalyst, followed by large sections packed only with adsorbent does not improve the conversion, showing that the advantages of the system come from the coupling of the reaction and separation.

Model Reaction

While the previous analysis indicates significant promise for the RFCR, the relative complexity of the phenomena involved requires experimental verification. A candidate model reaction for this study should satisfy most of the following criteria: (a) it should be an equilibrium-limited reaction, preferably with first-order or pseudo first-order kinetics to simplify the analysis; (b) Product and reactant must have different adsorption properties, with the reactant being preferably adsorbed on the adsorbent; (c) The adsorbent should have high capacity and good adsorption kinetics; (d) Reaction kinetics and adsorption isotherms have already been established; (e) To provide a benchmark, the reaction should, preferably, have been used in other reaction-separation systems.

The hydrogenation of 1,3,5-trimethylbenzene (Mesitylene, MES) to trimethylcyclohexane (TMC) was selected as a test reaction. This reaction was used by Fish and Carr (1989) and Ray and Carr (1995) in the investigation of CMCR and SMBCR, respectively, and can be used to benchmark the system. Hydrogen is fed in excess with nitrogen so that the reaction is pseudo first-order on mesitylene. The separation and reaction are feasible at the same temperature, and the hydrogen/nitrogen mixture required to carry out the reaction doubles as carrier for the adsorptive separation. The equilibrium conversion of MES to TMC in excess hydrogen (25% v/v in

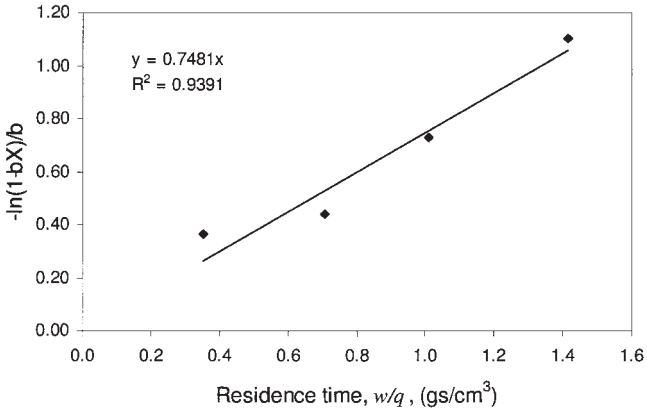

Figure 8. Experimental determination of forward reaction rate for the hydrogenation of MES at 190°C in a PFR ($b = 1 + 1/K_e$, hydrogen to MES mol ratio = 25, atmospheric pressure, 25% hydrogen in carrier).

nitrogen) is about 40% at 200°C, and 62% at 190°C according to Egan and Buss (1959). No side reactions are observed, and the only measurable product is TMC. The reaction rate constant on the catalyst, 2% platinum over alumina, mesh 80/100, was measured by placing 0.4 g of catalyst in a 0.475 cm inner dia. stainless steel plug-flow reactor placed inside a tube heater. The exit conversion was measured using a gas chromatograph (described in the section entitled "Experimental Apparatus"), and from the conversion data the reaction rate constant at 190°C was measured as $k_f = 0.75$ cm^3/gs, as shown in Figure 8.

Activated alumina and Chromosorb 106, supplied by Cobert Associates, are suitable adsorbents to separate MES and TMC according to Ray and Carr (1995). Both adsorbents were tested, injecting pulses of TMC, MES, and mixtures of both on packed columns of 0.3175 cm in dia. and 0.356 m long using helium as carrier in a Shimadzu 9A gas chromatograph with a flame ionization detector (FID). A large degree of peak trailing was observed for both components. At a flow rate of 47 cc/min, the retention times of MES and TMC on Chromosorb 106 were 3.55 and 2.16 min, respectively, showing poor separation of the peaks. On alumina, the retention times were 5.31 min for MES and 1.77 min for TMC, with good separation of the peaks yielding in a separation factor $\gamma = 3.06$ and $K'_{MES} = 175$. Alumina was, therefore, chosen as the adsorbent. When using alumina, injecting different pulse sizes of MES (0.2 μL to 50 μL) showed a decrease in the peak time as the injection pulse size increased (Table 1), indicating that the isotherm is not linear. Using the method of characteristics for the desorption process as described by Sherwood et al. (1975), a noncompetitive Langmuir isotherm was obtained for both components. In this method, the adsorbent is saturated with the adsorbate, and suddenly the adsorbate feed is stopped. The slope of the adsorption isotherm can be obtained from the desorption curve utilizing

$$\frac{\partial n}{\partial C} = \frac{\varepsilon}{\rho_B}\left[\frac{tv}{L} - 1\right] \tag{19}$$

where ρ_B is the adsorbent bulk density, v is the carrier superficial velocity, L is the column length, and t is the time elapse since the beginning of the desorption step. The method neglects mass-transfer resistances and longitudinal dispersion. Further details are given in Viecco (2004). The isotherms obtained for MES and TMC over alumina at 190°C are

$$\frac{n_{MES}(\text{mmol/g})}{0.0797} = \frac{2008C_{MES}(\text{mmol/cm}^3)}{1 + 2008C_{MES}(\text{mmol/cm}^3)} \tag{20.a}$$

$$\frac{n_{TMC}(\text{mmol/g})}{0.0827} = \frac{625C_{TMC}(\text{mmol/cm}^3)}{1 + 625C_{TMC}(\text{mmol/cm}^3)} \tag{20.b}$$

Experimental Apparatus

For laboratory-scale experimental studies, the most convenient way to configure a RFCR is a packed bed consisting of two stainless steel columns (1.05 cm inner dia. 0.304 m long), with reactant entry at the union of both columns. A solid state time delay relay (Dayton Electronics, Niles, IL, model 6A855) controls a set of four two way solenoid valves (ASCO, Florham Park, NJ, model EF8262G7) to periodically reverse the flow of the carrier. The columns are placed inside a tube heater (Lindberg, Waterford, WS, model 70S), whose temperature is controlled in three different sections. Liquid MES is injected by a syringe pump (Sage Instruments, Cambridge, MA, model 341B), which vaporizes instantly as it enters the tube heater before entering the reactor. Flow control is achieved by two mass flow controllers (Brooks, Hatfield, PA, model 5815), one for hydrogen and one for nitrogen. The exit stream is condensed in a cold trap operating at −25°C. The cold trap consists of a constant temperature bath (MGW Lauda, Germany, model RC20) filled with a mixture of ethylene glycol and water, a 0.350 m long stainless steel condenser, and a 500 mL glass flask to collect the condensed sample. Six type K thermocouples (0.156 cm in dia.) are placed throughout the column. The thermocouples are placed 0.101 m apart, perpendicular to the carrier flow and half way through the reactor diameter, with the two located near the inlet/outlet at 0.051m from the end of the column. Temperature data is collected and analyzed using a PC with a data acquisition system using Labtech Notebook software. The experimental setup is shown in Figure 9.

The cold trap efficiency was evaluated by injecting samples of MES/TMC of known concentration and then collecting them at the cold trap. For samples of 76, 62 and 42% TMC, the concentration of the collected samples was 75, 60, and 39%, respectively. This is a reasonable result since TMC has a lower boiling point than MES. These results mean that the conversion calculated from the collected samples will slightly underestimate the conversion.

Table 1. Retention Times for Different Injection Pulse Sizes for MES over Alumina 190°C and Helium Flow Rate of 47 cc/min

Injection pulse (μl)	0.2	0.5	1.0	3.1	6.2	10	30	50
Retention time (min)	6.74	5.98	5.31	3.33	2.94	2.34	1.25	0.86

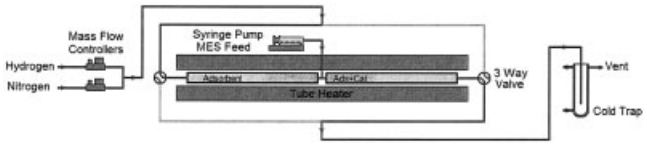

Figure 9. Experimental setup for the hydrogenation of MES in a RFCR.

The MES (MW = 102.2 g/mol, ρ = 0.865 g/mL), and TMC used in the experiments are 99%+ purity, supplied by Sigma-Aldrich. The adsorbent is activated alumina, Alcoa type F1, mesh 60/80, supplied by Cobert Associates (St. Louis, MO), and the catalyst is 2% $^{w}/_{w}$ platinum over alumina. Finally, the collected samples from each experimental run were analyzed using a Shimadzu 9A Gas Chromatograph equipped with a flame ionization detector (FID). Samples were quantitatively analyzed using a HP-1, 30m × 0.53mm capillary column, and helium as the carrier with the column temperature at 150°C.

Experimental results and discussion

Each experimental run was carried out for 20 h. Once the catalyst is reduced and the reactor is at 190°C, flow reversal and MES flow is started. Five hours after the run begins, a flask is placed in the cold trap and sample collection begins. 10 hours after the beginning of the run, the flask is removed with the average of t = 5 − 10 h of operation. Immediately a new flask is placed and the sample is collected. 20 hours after the start of the run, the second flask is removed and the sampled is labeled. The average conversion is determined from the composition of the second flask, corresponding to the last 10 h of the run. The cold trap acts as an integrator, while allowing 10 h to elapse from the beginning of the run to the point where the sample is collected allows the system to achieve cyclic steady state.

Six different conditions were used, labeled as sets 1 through 6, and different switching times were tested for each set. The conditions of each set are shown in Table 2, together with the highest average conversion obtained for each set. The packing configuration of the catalyst and adsorbent is shown in Figure 10. Sets 1 and 2 will study the effect of different packing configurations and amount of catalyst; set 3, the effect of reactant feed concentration; and sets 2 along with 4 through 6, the effect of carrier flow rate. The hydrogen percentage in the carrier mixture is decreased in sets 4 and 6 in order to maintain the same hydrogen partial pressure and, therefore, equilibrium conversion. All runs were carried out at 190 ± 1°C, and in all cases the effect of the cycle time was studied.

The effect of the switching time on the conversion is shown in Figure 11 for sets 1 and 2. The figure compares the conversion of the RFCR with the equilibrium conversion, the conversion of the same packed bed being operated as a plug-flow reactor with the reactant feed at the carrier inlet (PFR operation), and the conversion when the carrier and reactant feed are configured in the same way as the RFCR, but without changing the flow direction (PFR operation, half reactor). The conversion obtained for the RFCR for the switching times selected is well above that obtained for PFR operation. For switching times between 10 and 20 min for set 1 and 6 to 18 min for set 2, conversion is above the thermodynamic equilibrium. The maximum conversion is obtained at a switching time of 12 min, which corresponds to a dimensionless switching time of ~0.2, close to that predicted by the model. The dimensionless switching time is calculated according to Equation 12 using K'_{MES} = 209 obtained from the injection of a single pulse of MES in alumina.

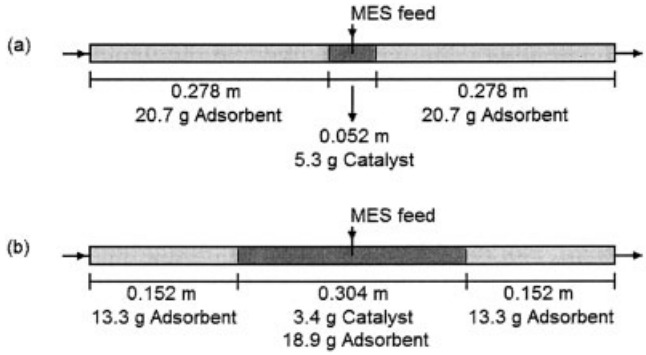

Figure 10. Adsorbent and catalyst packing in the RFCR experimental setup for (a) Set 1, and (b) Sets 2 through 6.

The experimental conversion increases as the switching time decreases, goes through a maximum and then decreases. This is the same trend predicted by the simple linear model, according to Figures 3 and 6. For long switching times the conversion should drop below the PFR operation conversion and approach that of the half reactor PFR operation. While this appears to be the trend, more data points at longer switching times are required in order to verify this claim.

A comparison between two different catalyst configurations (sets 1 and 2) can be made from Figure 11. In set 1, the catalyst is concentrated in the center of the reactor according to Figure 10a. In set 2, the catalyst is spread over half of the reactor, and it is physically mixed with the adsorbent. Spreading the catalyst over a larger section of the reactor, as in set 2, increases significantly the maximum conversion and the range of switching times that yield in conversion exceeding the thermodynamic equilibrium. Also important is that set 2 has a lower amount of catalyst,

Table 2. Experimental Conditions

	Set 1	Set 2	Set 3	Set 4	Set 5	Set 6
Carrier flow (cc/sec)	144	144	144	288	100	215
Hydrogen (%, dry)	25.0	25.0	25.0	21.2	25.0	23.1
Catalyst (g)	5.3	3.4	3.4	3.4	3.4	3.4
Adsorbent (g)	41.4	45.3	45.3	45.3	45.3	45.3
Damkohler	1.68	1.06	1.06	0.53	1.52	0.71
MES	0.49	0.49	0.20, 0.35, 0.74	1.0	0.35	0.74
Max. Conversion (%)	71.4	74.5	80.9	58.8	78.8	69.9

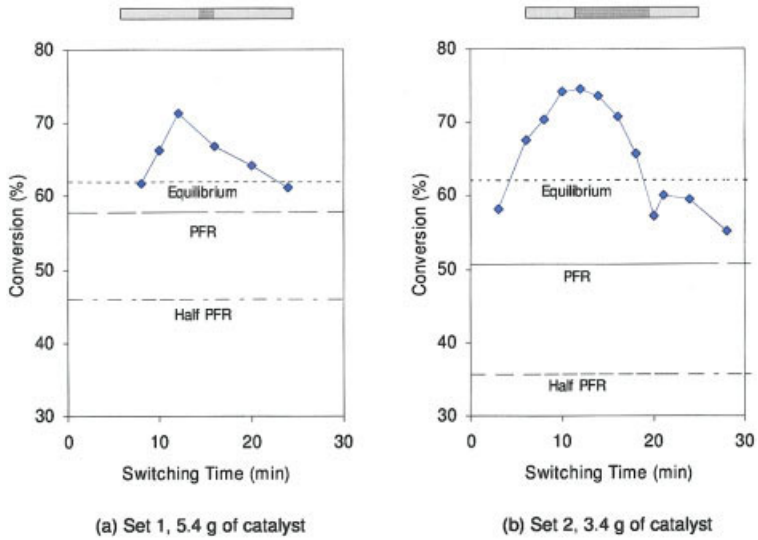

Figure 11. Average conversion as a function of the switching time for (a) set 1, and (b) set 2 compared to the equilibrium conversion and PFR operation.

The bar represents the packing configuration, where the light gray is adsorbent, and the dark gray is a mixture of adsorbent and catalyst. [Color figure can be viewed in the online issue, which is available at www.interscience.wiley.com.]

showing how the mixture of the adsorbent and catalyst has a significant advantage over a system where both are packed consecutively but not mixed. This behavior was predicted from the simple linear model, according to Figure 6. When the adsorbent and catalyst are mixed, the reactant concentration near the feed point is several times higher than the concentration that would be obtained if the carrier were mixed with the reactant in a steady-state reactor. This gives higher reaction rates and reduces the amount of catalyst required to achieve a certain degree of conversion to below that needed if the catalyst and adsorbent were not mixed. The same general trend observed for set 1 is seen for set 2, showing that the switching time is the most important parameter, confirming that the reactant is being trapped by adsorption. The maximum conversion occurs for the same switching time (12 min) in both sets, although for set 2 the conversion for 10 and 14 min is very close enough to that at 12 min. The conversion drops faster for set 2 than for set 1 as the switching time moves away from the optimum switching time, a trend explained by the lower amount of catalyst in this set. For longer switching times, this set also shows that the conversion approaches that of half-reactor operating as a PFR. For a switching time of 22 min, conversion is 42.6%, approaching the expected conversion of 35.6%.

The simple linear model previously described predicts that the performance of the RFCR is independent of the gas phase concentration, since the model assumes a linear adsorption isotherm. However, the system MES/TMC/Alumina is more closely described by the Langmuir adsorption isotherm described in the section entitled "Model Reaction", where the adsorption capacity of alumina is limited. In this case, the lower the reactant feed concentration, the more likely the RFCR will perform according to the linear model. Also, at lower feed concentrations, the reactant is better trapped, improving the conversion by increasing the reactant concentration inside the reactor. This effect is clearly seen in Figure 12, where the maximum conversion occurs at the lowest MES feed rate. At this reactant feed rate the conversion remains high for a larger range of switching times.

The final parameter to be considered is the flow rate of the carrier. Figure 13 compares the average conversion as a function of the dimensionless switching time for various flow rates. As the flow rate decreases, the Damkohler number increases. This should result in a higher conversion, since this increases the contact time between the catalyst and the reactant. The figure shows that the maximum conversion is achieved at the lowest flow rate, at a Damkohler of 1.52. According to the simulation results (Figures 4 and 7), the maximum conversion is obtained at a Damkohler of 1.5. Although this was not tested, further increasing the Damkohler number should result in a decrease of the maximum conversion.

The range of switching times that have a conversion exceeding the thermodynamic equilibrium is also the largest at the lowest flow rate tested. The conversion at the highest flow rate is below the thermodynamic equilibrium for all switching times tested.

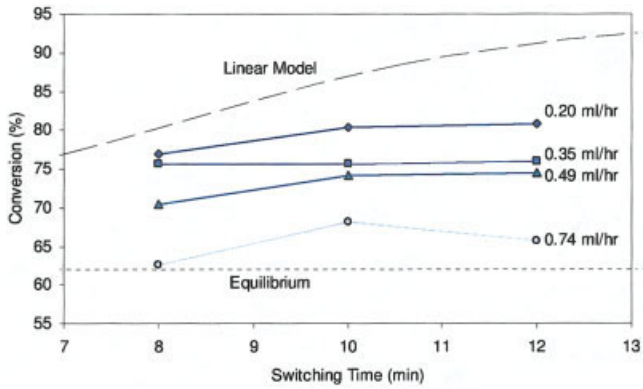

Figure 12. Effect of MES feed concentration (feed rate) on conversion (Set 3).

The parameters used in the simulation of the linear model data are Da = 1, N = 61, γ = 3, Ke = 1.63. [Color figure can be viewed in the online issue, which is available at www.interscience.wiley.com.]

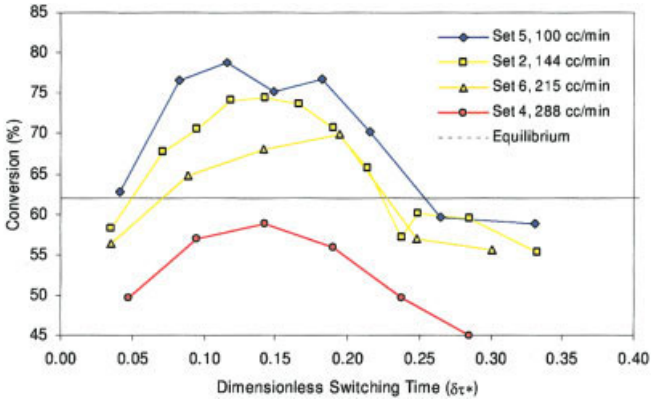

Figure 13. Effect of the carrier flow rate on the average reactor conversion.

[Color figure can be viewed in the online issue, which is available at www.interscience.wiley.com.]

According to the linear model, a conversion exceeding the thermodynamic equilibrium should be obtained even for this case (set 4, 288 cc/min, Da = 0.54). At a high flow rate, the resulting decrease in both the reactant concentration and the residence time would yield the observed decrease of conversion. It is important to notice that although the conversion (58.8%) was only slightly lower than the thermodynamic equilibrium (62%), it was higher than if the reactor was operated as a PFR (35.6%).

Comparison with the SMBCR

Ray and Carr (1995) reported their results on the experimental hydrogenation of MES on a simulated moving-bed chromatographic reactor (SMBCR). Their laboratory setup consisted of five columns (1.26 cm outer diameter, 0.305 m long), where two exit ports were used: one, located behind the feed point, collected unreacted MES; the second, located after the feed point, collected a mixture of MES and TMC. The use of two exit ports yielded a higher purity TMC stream and improved conversion. Since two different exit ports were used, two different carrier flows were also involved. Their experiments used Chromosorb 106, which according to their results presented better adsorption characteristics than alumina (γ = 3.2), and 0.74% platinum over alumina as catalyst. Each column was packed with a mixture of 10% catalyst and 90% Chromosorb 106 by weight. Assuming that the densities of Alumina and Chromosorb are comparable, it can be calculated that the amount of adsorbent was 21.4 g, and the amount of catalyst was 2.4 g in each bed, for a total of 108 g of adsorbent and 12 g of catalyst. The flow rate of hydrogen used was 50 cm^3/min, the flow rate of nitrogen was 60 cm^3/min, the hydrogen to MES feed ratio was 10, and the switching time used was 5 min. The reported conversion for the best experimental run was 82.5%, with a TMC purity of 94.6%.

A comparison between the two experiment setups shows the simplicity of the RFCR. The amount of valves, piping, and temperature control are significantly reduced. The amount of adsorbent used in the RFCR experiment was 42% of the amount used in the SMBCR. The amount of catalyst used in the RFCR experiment was 76% of the amount used in the SMBCR after accounting for the difference in platinum content. The hydrogen to MES ratio was higher in the RFCR than in the SMBCR (25 vs. 11), with similar overall carrier flow rates compared to set 5. The maximum conversion for set 5 obtained was 78.8%, only 4.5% below the SMBCR performance, and the maximum conversion obtained in the RFCR was 80.9% at a higher flow rate (144 cm^3/min), only 1.9% below the SMBCR. Therefore, the RFCR configuration makes a much better use of the amount of catalyst and adsorbent, in a simpler system, with almost identical results.

Comparison with model results

Only the simple linear model, the competitive equilibrium Langmuir model and the linear mass-transfer model will be evaluated. Figure 14 shows the competitive Langmuir model against the experimental results for Sets 2 and 3, together with the results from the simple linear equilibrium model. In this set, and for all other experimental sets, the linear equilibrium model significantly overpredicts the conversion. It provides, however, a good estimate of the optimal switching time.

For values of $k_{ads} = 10^5$ cc/(mmol.min), the model results have become independent of the value of k_{ads}, and the mass-transfer coefficient is large enough for adsorption equilibrium to be assumed. Using the adsorption data given by Eqs. 20a and 20b, but assuming a competitive Langmuir isotherm together with the model given by Eq. 16a–d, the effect of the feed concentration c_0 is shown in Figure 14. At low values of c_0 ($c_0 = 4.08 \times 10^{-8}$ mmol/cc), with low-surface saturation, the conversions approach the linear model results. As the feed concentration increases the adsorbent saturates, and its ability to capture the reactant decreases. The overall conversion decreases and more frequent switching is required to minimize the amount of reactant escaping the reactor. For Set 2 ($c_0 = 4.08 \times 10^{-4}$ mmol/cc) the model predicts correctly the maximum conversion, but, the optimal switching frequency is about half of the observed (6 min vs. 12 min), indicating shortcomings in the model. Figure 14 also shows the effect of the feed concentration as studied in Set 3. While the trends are correct, an increase in feed concentration will reduce the conversion and as for the concentration of Set 2, the conversion data are shifted to the right of the model prediction.

If the saturation of the surface is neglected ($\theta_i = 1$), the linear mass-transfer model is obtained and an analytical solution is possible. Figure 15 shows the effect of k_{ads} on the conversion. As expected at large k_{ads} (10^5 cc/(mmol.min)), the linear model

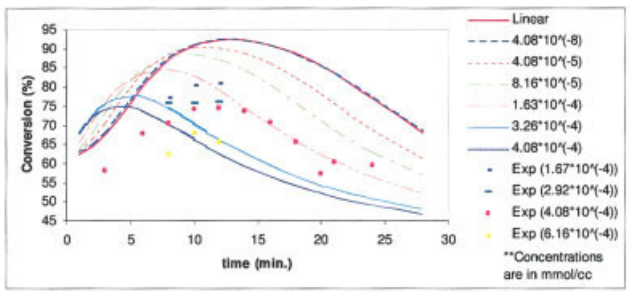

Figure 14. Effect of reactant concentration on the Langmuir model (N = 51) for Set 2/3. The experimental concentration is $4.08*10^{-4}$ mmol/cc.

[Color figure can be viewed in the online issue, which is available at www.interscience.wiley.com.]

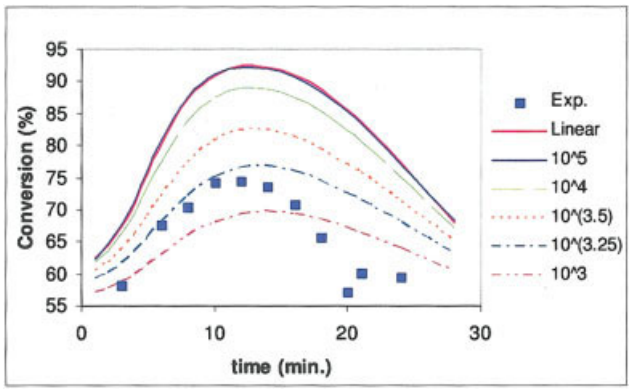

Figure 15. Effect of k_{ads} on the Linear Mass-transfer model (N = 51) for Set 2.

The closest match to the experimental data was determined to be $k_{ads} = 10^{3.25}$ cc/(mmol.min)≈1780 cc/(mmol.min). [Color figure can be viewed in the online issue, which is available at www.interscience.wiley.com.]

conversions are recovered. As k_{ads} decreases the conversion decreases while the optimal switching time remains the same. A reasonable fit of the experimental data is obtained for k_{ads} = 1780 cc/(mmol.min), although the model overestimates the conversions for short and long switching times. The same parameter provides an adequate fit of the experimental data of sets 1,3 – 6 as is shown in Figure 16.

Conclusions

The RFCR yields conversions that exceed the steady-state thermodynamic equilibrium conversion and achieves higher reaction rates than conventional reactors, such as a plug-flow reactor. The experimental results show that mixing the adsorbent and catalyst improves the conversion over a system where they are segregated, and it increases the robustness of the system in terms of the switching times, where conversion is higher than the thermodynamic equilibrium. Low flow rates or large amounts of catalyst improve the conversion of the system. The use of low-reactant concentration yields higher product concentration due to the better adsorption characteristics at low-concentrations for the isotherm studied. All these effects, predicted by the simple linear model, are confirmed by the experimental results.

The effect of the switching time and the switching time that corresponds to the maximum conversion are also in agreement between the simple linear model and the experimental results. A more detailed model including a competitive Langmuir isotherm and interfacial mass-transfer resistance, the latter being an adjustable parameter, was also studied. The best fit was obtained by a model that assumes interfacial mass-transfer resistance with a linear adsorption isotherm,which may indicate adsorption mass-transfer control.

The comparison between the SMBCR and the RFCR shows the robustness of the RFCR and how it can achieve a very similar performance to the SMBCR with a much simpler system. The RFCR requires that the reactant be preferably adsorbed with respect to the products. This is not a limitation for the SMBCR, where either products or reactants may be selectively adsorbed. However, if the products are adsorbed, the SMBCR requires an extra desorption step. Also, the ability of having multiple exit ports in the SMBCR is not available in the RFCR; therefore, only increases in overall conversion, and not purity can be obtained for this type of reactor. Increases of purity are possible by splitting the exit stream in different periods of time since only in the last moments before the carrier flow is reversed, the reactant is able to escape.

Notation

c_0 = feed concentration, mmol/cm^3
$c_{j,i}$ = gas phase concentration of component j in stage i, mmol/cm^3
$C_{j,i}$ = dimensionless gas phase concentration
c_{max} = maximum solid phase concentration, mmol/cm^3
Da_{ads} = $V_l \varepsilon\, k_{ads}\, c_{max}/q$ = adsorption Damkohler number
k_{ads} = interfacial mass transfer coefficient, cm^3/mmol.min
$\hat{n}_A$ = molar feed rate of reactant A, mmol/min
$n_{j,i}$ = solid phase concentration of component j in stage i, mmol/cm^3
v = void fraction factor
V = reactor volume, cm^3
q = carrier flow rate, cm^3/min

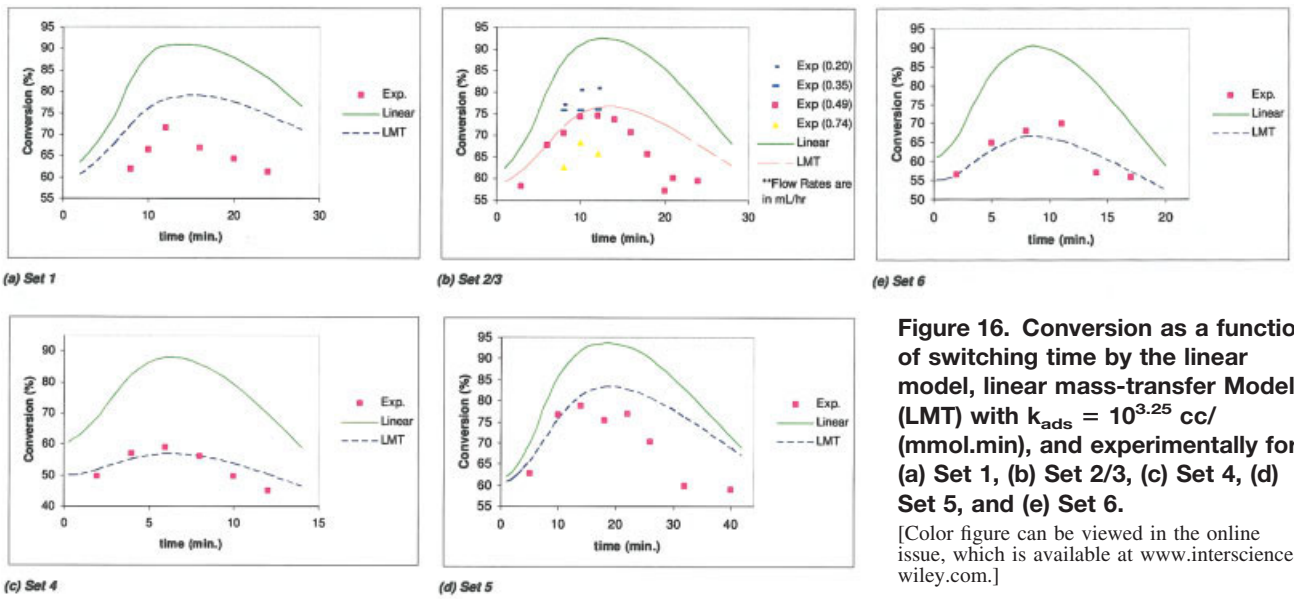

Figure 16. Conversion as a function of switching time by the linear model, linear mass-transfer Model (LMT) with $k_{ads} = 10^{3.25}$ cc/(mmol.min), and experimentally for (a) Set 1, (b) Set 2/3, (c) Set 4, (d) Set 5, and (e) Set 6.

[Color figure can be viewed in the online issue, which is available at www.interscience.wiley.com.]

t_s = half cycle time, min
k_f = forward reaction rate constant, s^{-1}
K_j = adsorption equilibrium constant of component j
ε = void fraction
$K_j' = \varepsilon+(1-\varepsilon)K_j$
$\gamma = K_A'/K_B'$ = separation factor
N = number of equilibrium stages
N_{cff} = number of equilibrium stages with admixture catalyst and adsorbent
K_e = reaction equilibrium constant
$Da = k_f V/q$ = Damkohler number
$\delta\tau^* = t_s q/VK_A'$ = dimensionless switching time, defined in eqn. 12.
$\tau^* = tqN/\varepsilon V$ = dimensionless switching time, defined in eqn. 17a.
θ_i = fraction of free adsorption sites
$\theta_{j,i}$ = dimensionless solid phase concentration

Literature Cited

Agar D., and Ruppel W., "Extended Reactor Concept for Dynamic DeNOx Design," *Chem. Eng. Sci.,* 43, (8), 2073-2078, (1988).

Egan, C. J., and W. C. Buss, "Determination of the Equilibrium Constants for the Hydrogenation of Mesitylene. The Thermodynamic properties of the 1,3,5-Trimethylcyclohexanes." *J. Phys. Chem*., 63, 1887-1890, (1959).

Falle, S., J. Kallrath, B. Brockmuller, A. Shreieck, J. Griddings, D. Agar, and O. Watzenberger, "The Dynamics of Reverse Flow Chromatographic Reactors with Side Stream Feed," *Chem. Eng. Comm*. 135, 185-211, (1995).

Fish, R. Carr, An Experimental Study of the Countercurrent Moving Bed Chromatographic Reactor," *Chem. Eng. Sci*., 44 (9), 1773-1783, (1989).

Jeong, Y.O., and D. Luss, "Pollutant Destruction in a Reverse-Flow Chromatographic Reactor," *Chem. Eng. Sci*., 58 (7), 1095-1102, (2003).

Ray, A. J., and R. Carr, "Experimental Study of a Laboratory Scale Simulated Counter Current Moving Bed Chromatographic Reactor," *Chem. Eng. Sci*., 50 (14), 2195-2202, (1995).

Sherwood, T. K., R. L Pigford, and C. R. Wilke, "Mass Transfer," McGraw Hill, 1975.

Viecco, G. A., "The Reverse Flow Chromatographic Reactor," PhD Dissertation, Lehigh University, (2004).

Viecco, G. A., and Caram H. S., "The Reverse Flow Chromatographic Reactor", *AIChE J*, 50(9), 2266 (2004).

Manuscript received June 1, 2004, and revision received Dec. 23, 2005.